

Cage Size and Jump Precursors in Glass-Forming Liquids: Experiment and Simulations

Raffaele Pastore,^{*,†} Giuseppe Pesce,[‡] Antonio Sasso,[‡] and Massimo Pica
Ciamarra^{¶,†}

[†] *CNR-SPIN, sezione di Napoli, Dipartimento di Fisica, Campus universitario di Monte S.
Angelo, Via Cintia, 80126 Napoli, Italy*

[‡] *Dipartimento di Fisica, Università di Napoli Federico II, Campus universitario di Monte
S. Angelo, Via Cintia, 80126 Napoli, Italy*

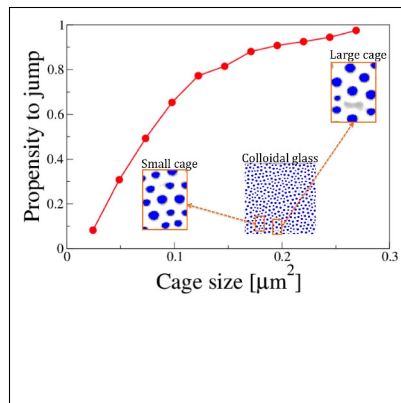
[¶] *Division of Physics and Applied Physics, School of Physical and Mathematical Sciences,
Nanyang Technological University, Singapore*

E-mail: raffaele.pastore@spin.cnr.it

Abstract

Glassy dynamics is intermittent, as particles suddenly jump out of the cage formed by their neighbours, and heterogeneous, as these jumps are not uniformly distributed across the system. Relating these features of the dynamics to the diverse local environments explored by the particles is essential to rationalize the relaxation process. Here we investigate this issue characterizing the local environment of a particle with the amplitude of its short time vibrational motion, as determined by segmenting in cages and jumps the particle trajectories. Both simulations of supercooled liquids and experiments on colloidal suspensions show that particles in large cages are likely to jump after a small time-lag, and that, on average, the cage enlarges shortly before the particle jumps. At large time-lags, the cage has essentially a constant value, which is smaller for longer-lasting cages. Finally, we clarify how this coupling between cage size and duration controls the average behaviour and opens the way to a better understanding of the relaxation process in glass-forming liquids.

Graphical TOC Entry



Molecular liquids on lowering the temperature and colloidal suspensions on increasing the volume fraction exhibit a glass transition from a liquid-like to an amorphous solid-like state.¹⁻⁶ On approaching this transition, the dynamics becomes intermittent and shows large spatio-temporal fluctuations, also known as dynamic heterogeneities.^{7,8} These dynamic features are currently emerging as a common hallmark of many complex systems, such as foams, gels⁹ and fiber networks¹⁰ as well as biological materials, such as cell tissues^{11,12} and microswimmers,¹³ in which primary particles move in a crowded environment. As a consequence, there is a great deal of interest in applying concepts developed by the glass community to understand the behavior of these systems. As telling example, recent results show that the degree of dynamic heterogeneities highlight and allow rationalizing pathological conditions in epithelial cell tissues.^{11,12}

In glass-forming liquids, the dynamics is spatio-temporal heterogeneous since the probability that a particle rearranges in a given time interval is not spatially uniform, as long as the considered time interval is smaller than the relaxation time. Since the local environment of a particle affects its short time motion, dynamic heterogeneities indicates the presence of structural heterogeneities. This observation triggered a resurgence of interest^{14,15} in the search of connections between structure and dynamics in supercooled liquids, a notorious difficult task. This problem can be somehow simplified assuming the structure to influence the short time dynamics, and the short time dynamics to influence the relaxation process. Thus, instead of looking for connections between structure and long time dynamics, one looks for connections between short time dynamics and relaxation. Research in this direction clarified that particles highly mobile on a short time scale are also those that most probably will undergo a significant displacement on the structural relaxation timescale. Operatively, particles highly mobile on a short time scale can be identified, somehow equivalently, as those located where soft vibrational modes are localized,¹⁶⁻¹⁸ as those in regions with small local elastic constants,¹⁹ as those with a large free volume,²⁰ and as those having a large vibrational motion.^{21,22} While the existence of an interplay between short time dynamics

and structural relaxation is clear,²³ quantitative relations between these two features, at the single particle level, are still lacking.

Here we tackle this issue through a combined experimental and numerical study of two popular fragile glass-forming models, we have investigated in previous works.^{24–27} Briefly, we perform *i*) experiments on a nearly two-dimensional suspension of hard-sphere colloids, whose dynamics slows down on increasing the volume fraction, and, *ii*) molecular dynamic simulations of a two dimensional system of soft disks, whose dynamics slows down on lowering the temperature (see Methods for details on the investigated systems). By taking advantage of the intermittent cage-jump motion characterizing the single-particle dynamics in supercooled liquids and glasses,^{28–35} we segment the particle trajectories in cage and jumps²⁴ and use the cage size as a proxy of the short time motion of a particle; similarly, we use jumps as proxies of the local relaxation.

As a nearly instantaneous measure of the cage size at time t , we use the fluctuations S_C^2 of the particle position in a short time interval $[t - \delta t/2, t + \delta t/2]$, with δt of the order of the Debye-Waller factor characteristic time.²³ Further details on the cage-jump detection algorithm and on the cage size estimate are discussed in Methods. For a particle in a cage of size S_C^2 at time t , we consider the conditional probability distributions, $P_{CC}(S_C^2, \Delta t)$, that the particle stays permanently caged up to $t + \Delta t$, and, $P_{CJ}(S_C^2, \Delta t)$, that the particle starts jumping at time $t + \Delta t$. These conditional probabilities do not depend on t as the systems we consider are in thermal equilibrium, and, therefore, invariant under time translations. For every Δt , the conditional probabilities are normalized, $\int P_{CC}(S^2, \Delta t) dS^2 = \int P_{CJ}(S^2, \Delta t) dS^2 = 1$.

The influence of the cage size at time t on the probability that a particle will start jumping at later time $t + \Delta t$ can be quantified introducing a jump propensity, $\Pi_J(S_C^2, \Delta t)$,

$$\Pi_J(S_C^2, \Delta t) = \frac{P_{CJ}(S_C^2, \Delta t)}{P_{CC}(S_C^2, \Delta t) + P_{CJ}(S_C^2, \Delta t)}. \quad (1)$$

When the probability that a particle jumps is not correlated to the size of its cage, $\Pi_J(S_C^2, \Delta t) =$

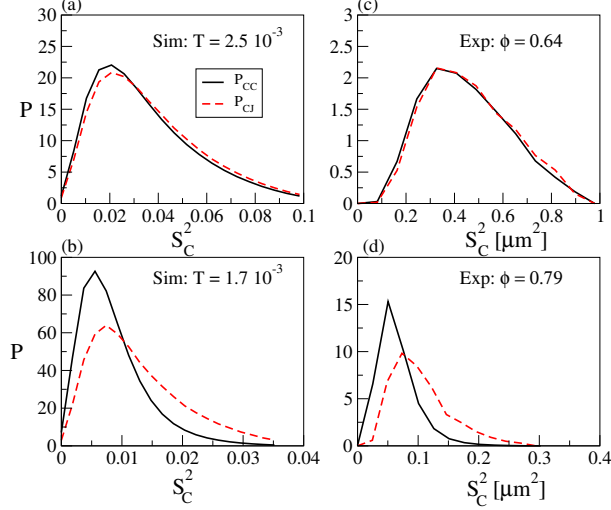


Figure 1: Conditional probability distributions, $P_{CC}(S_C^2, \Delta t)$ and $P_{CJ}(S_C^2, \Delta t)$, as a function of the cage size S_C^2 and at a short time-lag, $\Delta t = \delta t$. Panel a and b: simulations at the lowest and the highest investigated temperature, respectively. Panel c and d: experiments at the largest and the smallest investigated volume fraction, respectively.

$\Pi_{\text{dec}} = 1/2$. Conversely, $\Pi_J(S_C^2, \Delta t) \simeq 0$ and $\Pi_J(S_C^2, \Delta t) \simeq 1$ indicate that particles with cages of size S_C^2 are very unlikely and very likely to jump after a time Δt , respectively.

Jump propensity at short times. To investigate how the cage size correlates with the probability that a particle is about to jump, we start by considering a time-lag, $\Delta t = \delta t$, that is the smallest time to probe $S_C^2(t)$ and $S_C^2(t + \Delta t)$ over non-overlapping time windows, according to our cage-jump algorithm. Physically, we are investigating correlations separated by a timescale fixed by the Debye-Waller factor time. Fig. 1 illustrates our numerical and experimental results for the conditional probability distributions P_{CC} and P_{CJ} . In the numerical simulations, we observe the two distributions to be almost indistinguishable at high temperature (panel a). Conversely, clear differences emerge at low temperature (panel b), P_{CJ} having a much fatter tail than P_{CC} . Analogous results are observed in the experiment, when comparing the distributions measured at low and at high volume fractions, as in panels c and d.

This effect can be further quantified by the jump propensity, $\Pi_J(S_C^2, \delta t)$, of Eq. 1. The dependence of this propensity on the cage size is illustrated in Fig. 2. Panel a shows results

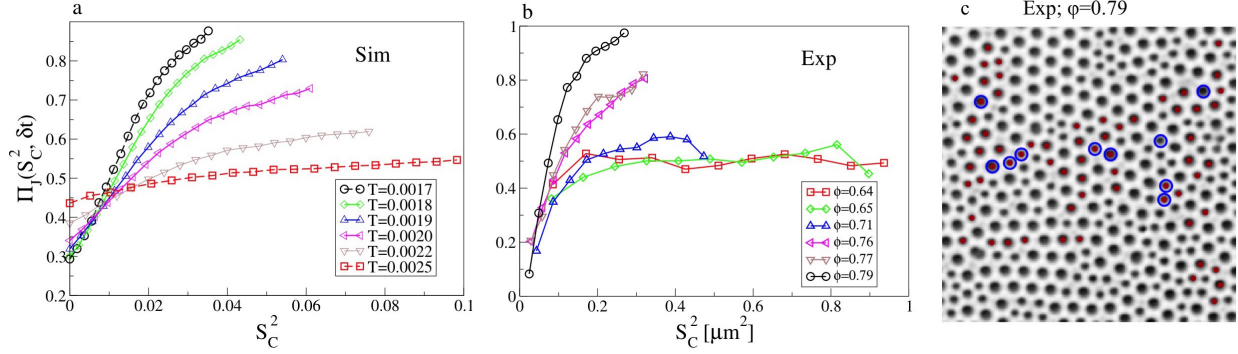


Figure 2: Dependence of the short-time jump propensity, $\Pi_J(S_C^2, \delta t)$, on the cage size, in the liquid and in the supercooled regime, in numerical simulations (a), and in the experiment (b). c) Snapshot of the investigated colloidal suspension at volume fraction $\phi = 0.79$, taken at a time $t = 0s$. Full red circles indicate caged particles with a large vibrational motion, ($S_C^2(t) > 0.1\mu m^2$), while empty circles surround the caged particles that will jump in the time interval $[30s, 150s]$.

for the numerical system at different temperatures, while panel b shows experimental results at different volume fractions. At high temperatures or low volume fraction, i.e. in the conventional liquid phase, no correlations are expected between the cage amplitude and the jumping ability of a particle, and indeed we do observe $\Pi_J(S_C^2, \delta t) \simeq \Pi_{dec} = 1/2$. Conversely, in the supercooled regime $\Pi_J(S_C^2, \delta t)$ is a growing function of S_C^2 , indicating that the larger the cage of a particle, the more likely the particle will jump after a short delay. It is worth noticing that, even for the most supercooled systems, the propensity is close to unity only for the largest cage size detected, whereas it seems to saturate at a progressively lower values as supercooling becomes more moderate.

From these figures we learn that, in the supercooled regime, particles with a large cage are more likely to start jumping after a short time-lag, although jumps originating from small cages are still possible. Figure 2c provides a direct visualization of this effect for the colloidal systems we have investigated. The figure is a snapshot of the system in a deeply supercooled state (the highest investigated volume fraction) and highlights that a large fraction of the jumps, occurring shortly after the considered frame, do originate from large cages. However, there also a few jumps originating from small cages, as well as, many large cages not giving

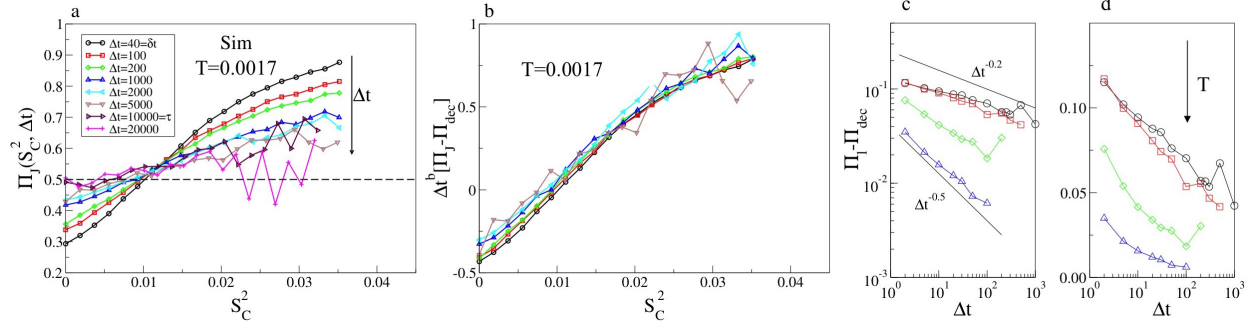


Figure 3: Panel a illustrates the dependence of the jump propensity on the cage size, at different time-lag Δt , as indicated. Data corresponding to different Δt can be collapsed on the same master functional form (see Eq. 2), as in panel b, suggesting a slow power-law decay of the temporal correlations. Data at the longest time-lags are too noisy and are not reported in this scaling. Panel c illustrates the excess jump propensity averaged over the 30% largest cages, $\Pi_l - \Pi_{dec}$, as a function of the time-lag, Δt , for simulations at different temperature. From top to bottom: $T = 1.7 \cdot 10^{-3}, 1.8 \cdot 10^{-3}, 1.9 \cdot 10^{-3}, 2.0 \cdot 10^{-3}$. Solid line indicates that the decay is compatible with a power law, the exponent decreasing on cooling, as indicated. Panel d reports the same data in a lin-log plot, clarifying that, at low temperature, the decay is also consistent with a logarithmic law.

rise to a jump on the considered timescale.

Jump propensity relaxation. In the limit in which Δt is much larger than the relaxation time, the probability that a particle jumps at time $t + \Delta t$ should not depend on the size of its cage at time t . Thus, for larger Δt one expects $\Pi(S_C^2, \Delta t) = \Pi_{dec} = 1/2$. Here we consider the relaxation dynamics of the propensity, $\Pi_J(S_C^2, \Delta t)$, by focusing on its Δt dependence. Fig. 3a illustrates numerical results obtained at low temperature, the experimental ones at high volume fraction being similar. As Δt increases, the propensity $\Pi(S_C^2, \Delta t)$ evolves and approaches $\Pi_{dec} = 1/2$, as expected. Fig. 3b supports the following scaling relation form for the Δt dependence of the propensity,

$$\Pi(S_C^2, \Delta t) = \Pi_{dec} + \Delta t^{-b} f(S_C^2) \quad (2)$$

with $f(x)$ a universal scaling function, and $b \simeq 0.2$. Thus, the decay of the jump propensity occurs through a slow power-law process.

The same decay process is seen to occur at other temperatures, with the exponent b increasing with T . This is shown in Fig. 3c, that reports the Δt dependence of $\Pi_l(\Delta t) - \Pi_{\text{dec}}$, Π_l being the propensity averaged over the largest cages (30%). In panel d, we illustrate the same data on a lin-log scale, to clarify that, at low temperature, a logarithmic behaviour also describes this decay.

Cage dynamics. Since the jump propensity depends on the cage size, the jump of a particle might be preceded by an enlarging of the cage, possibly driven by changes in the local structure. Here we consider this issue investigating the time evolution of the cage size.

For each cage of duration $t_{w,i}$ and end time $t_{J,i}$ (where a jump starts), we monitor the cage size $S_{C,i}^2(\Delta t)$ as a function of the time left before the jump, $\Delta t = t_{J,i} - t$, with $t \in [t_{J,i} - t_{w,i}, t_{J,i}]$. We first consider the average cage size of all particles that start a jump after a same time-lag Δt :

$$\langle S_C^2(\Delta t) \rangle = \frac{\sum_i S_{C,i}^2(\Delta t) \Theta(\Delta t - t_{w,i})}{\sum_i \Theta(\Delta t - t_{w,i})} \quad (3)$$

where the sums runs over all the detected cages and the Heaviside function, Θ , accounts for the fact that, at a given Δt , only cages with $t_{w,i} > \Delta t$ do contribute to the average.

Figure 4a shows $\langle S_C^2(\Delta t) \rangle$ at the lowest investigated temperature in simulations, clarifying that the average cage size changes in time significantly. At relatively small Δt , a smooth but clear grow of $\langle S_C^2(\Delta t) \rangle$ takes place as Δt vanishes, which is the signature of a cage-opening process preceding a jump. For $\Delta t \gtrsim 100$, this trend becomes less marked, but survives up to long time, since $\langle S_C^2(\Delta t) \rangle$ monotonically increases as Δt decreases, with a seemingly logarithmic behaviour. This is a quite counter-intuitive result, as the cage dynamics is expected to be stationary at least well before a jump starts, and, therefore, should likely lead to a long-time plateau in $\langle S_C^2(\Delta t) \rangle$. To rationalize this result and reconcile it with the standard cage picture, we consider that the cage duration is characterized by a broad distribution, $P(t_w)$, also known as waiting time distribution, which decays as t_w increases.^{24,25,27} Since the value of $\langle S_C^2(\Delta t) \rangle$ is only determined by those cages of duration $t_w > \Delta t$, we speculate that the behavior of $\langle S_C^2(\Delta t) \rangle$ could be explained assuming cages

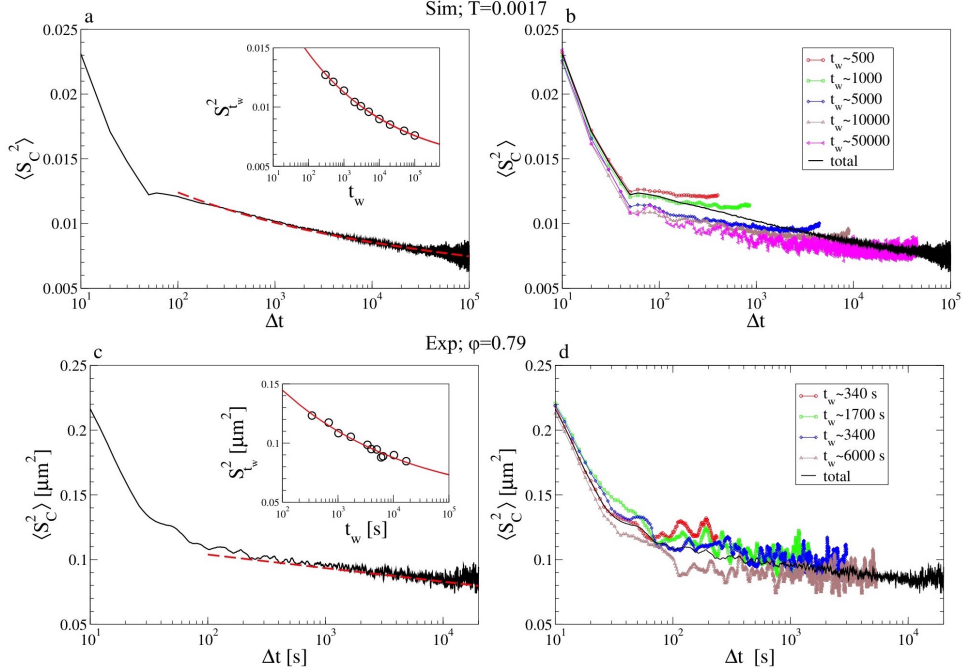


Figure 4: From simulations at the lowest investigated temperature a) cage size averaged over the total ensemble of cages, $\langle S_C^2(\Delta t) \rangle$ (solid line). At long time, data are correctly approximated by numerically computing the model of Eq. 5 (dashed line), using a stretched exponential fit for $P(t_w)^{27}$ and the fit for $S_{t_w}^2$ as reported in the inset. b) Cage size averaged over the total ensemble of cages (line) and over sub-ensembles of cages of fixed lifetimes t_w (line-points). Upper Inset: $S_{t_w}^2$ as a function of t_w , as obtained by a constant fit to the long-time behaviour of $\langle S_C^2(\Delta t) \rangle_{t_w}$. The solid line is a fit to the data, $S_{t_w}^2 = A/t_w^\beta + S_\infty$, with $A = 0.02 \pm 0.001$, $\beta = 0.18 \pm 0.01$, $S_\infty = 0.0047 \pm 0.0001$. Panels c), d) and the lower Inset reported the same analysis for experiments at the largest investigated volume fraction. The fitted parameters in the inset are $A = 0.23 \pm 0.01$, $\beta = 0.19 \pm 0.01$, $S_\infty = 0.047 \pm 0.001$

with different t_w to have a different dynamics. To confirm this hypothesis, we compute the average size, $\langle S_C^2(\Delta t) \rangle_{t_w}$, over sub-ensembles of cages with a fixed lifetime t_w (to improve statistics, $\langle S_C^2(\Delta t) \rangle_{t_w}$ is operatively computed as the average over all cages with waiting time in the range $t \in [t_w - t_w/10, t_w + t_w/10]$). Figure 4b compares $\langle S_C^2(\Delta t) \rangle_{t_w}$, for a number of t_w , with the total average $\langle S_C^2(\Delta t) \rangle$. At small Δt , curves corresponding to different t_w overlap, indicating that the cage opening process is not affected by t_w . Away from the jump, instead, results do depend on the cage duration. Indeed, $\langle S_C^2(\Delta t) \rangle_{t_w}$ attains a roughly Δt independent value, $S_{t_w}^2$, which is smaller for larger t_w . The upper inset of Fig. 4a shows the estimated values of $S_{t_w}^2$ as a function of t_w , suggesting that the data are compatible with a

power law plus a constant term, $S_{t_w}^2 = A/t_w^\beta + S_\infty^2$.

We have performed the same analysis for the experimental system, finding fully consistent results as in Fig. 4c and d, although the sub-ensemble averages $\langle S_C^2(\Delta t) \rangle_{t_w}$ are much more noise, due to poorer statistics.

Overall, these results demonstrate the existence of a coupling between cage size and duration. In particular, one can assume that, for large Δt , the cage size, $\langle S_C^2(\Delta t) \rangle_{t_w}$, acquires a constant value determined by the overall cage duration, t_w . These results lead to a simple model to rationalize the apparently anomalous behaviour of the average cage size, $\langle S_C^2(\Delta t) \rangle$, at large Δt . Indeed, the average over the whole ensemble of cages can be written as weighted sum over sub-ensemble averages:

$$\langle S_C^2(\Delta t) \rangle = \frac{\sum_{t_w=\Delta t}^{\infty} \Omega(t_w) \langle S_C^2(\Delta t) \rangle_{t_w}}{\sum_{t_w=\Delta t}^{\infty} \Omega(t_w)} \quad (4)$$

where $\Omega(t_w)$ is the number of detected cages of lifetime t_w . Considering that this number is proportional to the waiting time distribution, $\Omega(t_w) \propto P(t_w)$, and that for large Δt , $\langle S_C^2(\Delta t) \rangle_{t_w} \simeq S_{t_w}^2$, Eq.4 finally reads:

$$\langle S_C^2(\Delta t) \rangle = \frac{\int_{t_w=\Delta t}^{\infty} P(t_w) S_{t_w}^2 dt_w}{\int_{t_w=\Delta t}^{\infty} P(t_w) dt_w} \quad (5)$$

which relates the cage size and the waiting time distribution for $\Delta t \gg 0$. In order to test this theoretical prediction, we have evaluated the r.h.s. of Eq. 5 using our estimation for $S_{t_w}^2$ and $P(t_w)$ as a function of t_w . The prediction, reported as a dashed line in Fig. 4a and Fig. 4c, describes very well the data for Δt larger than the cage opening process. Overall, these results suggest that the cage size only increases shortly before a jump occurs, whereas the apparent long-time grow of $\langle S_C^2(\Delta t) \rangle$ is the consequence of averaging over an ensemble characterized by a coupling between cage size and duration, as well as, by a broad distribution of cage duration.

In this paper, we have investigated the single particle motion in glass-forming liquids

to illuminate the relation between short-time dynamics of localized particles and rearrangements leading to the structural relaxation on much longer timescales. The novel strategy we have introduced and the fundamental nature of the considered models make this analysis directly applicable to a wide variety of biological, chemical and physical systems, in which particle crowding plays a major role. In particular, we focused on a nearly instantaneous dynamical property, the cage size, and explored its temporal evolution, as well as, the correlation with the following jumps. Through the investigation of a jump propensity, we have clarified that particles rattling in large cages are more likely to jump after a short delay than particles rattling in small cages. Accordingly, the process of cage opening consists, on average, in a smooth enlargement of the cage, which lasts over a short time interval preceding the jump. However, the correlation between jump propensity and cage size is only statistical, and progressively weakens as the time-lag between cage measurement and jump detection increases. We provided evidences that, at large time-lags, the cage size is essentially constant and is related to the overall duration of the cage itself, the smaller the cage the longer the cage duration. This coupling between cage size and duration suggests that cage size and local structural order are also intimately related. For example, in the model numerically investigated in this paper, the time a particle spends in its cage before jumping is found to be correlated with the local hexatic order²⁷ and, therefore, similar correlations should in turn exist between the cage size and the hexatic order. Accordingly, the higher the local order, the smaller the cage size and the longer the cage duration. A possible explanation for this effect is that particles trapped in small cages are those packed in the core of highly ordered regions. Particles in the core of these regions can jump only when reached by a diffusing structural defect and, therefore, after those of the periphery, resulting in larger cage duration. One such mechanism has been reported for experiments on charged colloidal suspensions⁴⁷ and simulations of glass-forming liquids.⁴⁸

A further remark concerns the impressive similarity of the reported results, that we have obtained by numerically investigating a molecular supercooled liquids and by experimentally

studying a hard-sphere colloidal suspension. Such a similarity supports the universal nature of the cage-jump motion^{27,29} and cannot be simply rationalized by the known dynamic scaling between hard and soft sphere systems, since this scaling is applicable to the family of soft potentials with inverse power-law dependence on the interparticle distance, $V(r) \propto 1/r^\nu$ (whose $\nu \rightarrow \infty$ limit corresponds to the hard sphere potential).^{49–52} This kind of dynamic equivalence does not hold for our supercooled liquid model, which is, instead, characterized by a soft harmonic potential, not diverging for $r \rightarrow 0$ and showing properties, that cannot be mapped on hard-sphere-systems.⁵³

While in this paper we investigate the correlation between the cage size and the first following jump, a possible extension of this work consists in considering subsequent jumps, that is, whether particles which have a large propensity to make a jump are also likely to make many subsequent jumps. This is a way to investigate the life-time of dynamic heterogeneity from a single particle perspective.⁴⁶ A closely related question is understanding to what extent it is possible to predict the jumps through measurement of the cage size at a previous time. Similar studies have been performed in numerical works using the isoconfigurational ensemble,^{16,21} but the possibility to make practical prediction in experimental systems is still an open issue.

Methods

Experimental. We have experimentally investigated a popular model system of hard-sphere colloidal glass-forming suspension.^{25,36–39} Precisely, the sample consists in a 50:50 binary mixture of silica beads dispersed in water, at nearly monolayer condition. Bead diameters are 3.16 ± 0.08 and $2.31 \pm 0.03 \mu\text{m}$ respectively, resulting in a ≈ 1.4 ratio known to prevent crystallization. We image the system using a standard microscope equipped with a 40x objective (Olympus UPLAPO 40XS). The images were recorded using a fast digital camera (Prosilica GE680). Particle tracking was performed using custom programs. We have investigated

different volume fractions ϕ , in the range 0.64–0.79, where the systems can be properly equilibrated. Increasing the volume fraction, the relaxation time, τ , measured on the typical jump length and at thermal equilibrium, increases in the interval $10^2 s \gtrsim \tau \gtrsim 3 \cdot 10^4 s$ and is compatible with a power-law functional form, $\tau(\phi) \propto (\phi_c - \phi)^{-c}$, with $\phi_c \simeq 0.81 \pm 0.01$ and $c = 2.6 \pm 0.02$. Further details on the systems and on the experimental set-up can be found in Ref.²⁵

Numerical simulations. We have performed NVT molecular dynamics simulations⁴⁰ of a popular glass-forming model.⁴¹ The system consists in a two-dimensional 50:50 binary mixture of $2N = 10^3$ disks, with a diameter ratio $\sigma_L/\sigma_S = 1.4$, known to inhibit crystallization, at a fixed area fraction $\phi = 1$ in a box of side L . Particles interact via a soft potential, $V(r_{ij}) = \epsilon ((\sigma_{ij} - r_{ij})/\sigma_L)^\alpha \Theta(\sigma_{ij} - r_{ij})$, with $\alpha = 2$ (Harmonic). Here r_{ij} is the inter-particle separation and σ_{ij} the average diameter of the interacting particles. This interaction and its variants (characterized by different values of α) are largely used to model dense colloidal systems, such as foams,⁴² microgels⁴³ and molecular glasses.^{17,44} Units are reduced so that $\sigma_L = m = \epsilon = k_B = 1$, where m is the mass of both particle species and k_B the Boltzmann's constant. The two species behave in a qualitatively analogous way, and all data presented here refer to the smallest component. In our simulations, the glass transition is approached by lowering the temperature in the range $T \in [1.7 \cdot 10^{-3}, 2.5 \cdot 10^{-3}]$. At each investigated temperature, we monitor the dynamics after fully equilibrating the systems. Lowering T , the relaxation time, τ , increases in the interval $2 \cdot 10^2 \gtrsim \tau \gtrsim 10^4 s$ and is well described by a super-Arrhenius, $\tau(T) \propto \exp(A/T^2)$, with $A = const.$ ²⁶

Cage-jump detection algorithm. The trajectory of each particle is segmented in a series of cages interrupted by jumps using an algorithm introduced in Ref.,²⁴ and largely tested both in simulations^{26,27,45} and experiments.²⁵ To identify caged and jumping particles the algorithm compares the fluctuations of the particle position at a given time to the Debye-Waller factor. To this end, we associate to each particle, at each time t , the fluctuations of its position, $S^2(t) = \langle r^2(t_0) \rangle - \langle r(t_0) \rangle^2$, averaged over the time interval $[t - \delta t/2, t + \delta t/2]$.

Following Ref.²³ we defined the Debye-Waller factor from the mean square displacement as $\langle u^2 \rangle = \langle r^2(t_{DW}) \rangle$, t_{DW} being the time where $d \log(\langle r^2(t) \rangle) / d \log(t)$ is minimal. δt is chosen of the order of t_{DW} , therefore being much smaller than the relaxation time, τ , but large enough for a particle to experiment several collisions with its neighbours. Accordingly, the algorithm is not sensitive to the single oscillation dynamics, which is ballistic for molecular liquids and diffusive for colloidal suspensions. Specifically, we use $\delta t = 40$ for simulations and $\delta t \simeq 60s$ for experiments, respectively. At time t , a particle is considered in a cage if $S^2(t) < \langle u^2 \rangle$, and jumping otherwise. When S^2 equals $\langle u^2 \rangle$, a particle is either starting or ending a jump/cage. This algorithm allows for easily estimating the cage duration, t_w , which is the time-lag between two subsequent jumps of the same particle. For a caged particle, a nearly instantaneous measure of the size of its cage at time t is, by construction, the fluctuation of the position at that time, $S_C^2(t) = S^2(t)$.

Acknowledgement

We acknowledge financial support from MIUR-FIRB RBFR081IUK, from the SPIN SEED 2014 project *Charge separation and charge transport in hybrid solar cells* and from the CNR–NTU joint laboratory *Amorphous materials for energy harvesting applications*. MPC acknowledges financial support from the Singapore Ministry of Education Academic Research Fund Tier 1 grants RG 104/15 and and RG 179/15.

References

- (1) Liu, A. J.; Nagel, S. R. Nonlinear dynamics: Jamming is not just cool any more. *Nature* **1998**, *396*, 21–22.
- (2) Trappe, V; Prasad, V.; Cipelletti, L.; Segre, P.N.; Weitz, D. A. Jamming phase diagram for attractive particles. *Nature* **2001**, *411*, 772-775.

- (3) Solomon, M. J.; Spicer, P. T. Microstructural regimes of colloidal rod suspensions, gels, and glasses. *Soft Matter* **2010**, *6*, 1391–1400
- (4) Debenedetti, P. G.; Stillinger, F. H. Supercooled liquids and the glass transition. *Nature*, **2001**, *410*, 259–267.
- (5) Capaccioli, S.; Paluch, M.; Prevosto, D.; Wang, L.-M.; Ngai, K. L. Many-body nature of relaxation processes in glass-forming systems. *J. Phys. Chem. Lett.* **2012**, *3*, 735–743.
- (6) Cervený, S.; Mallamace, F.; Swenson, J.; Vogel, M.; Xu, L.; Confined water as model of supercooled water. *Chem. Rev.* **2016**, *116*, 7608–7625.
- (7) Berthier, L.; Biroli, G.; Bouchaud, J.-P.; Cipelletti, L.; van Saarloos, W. *Dynamical heterogeneities in glasses, colloids, and granular media* Oxford University Press: Oxford, UK; 2011.
- (8) Grzybowski, A.; Koperwas, K.; Kolodziejczyk, K.; Grzybowska, K.; Paluch, M. Spatially heterogeneous dynamics in the density scaling regime: time and length scales of molecular dynamics near the glass transition. *J. Phys. Chem. Lett.* **2013**, *4*, 4273–4278.
- (9) Duri, A.; Sessoms, D. A.; Trappe, V.; Cipelletti, L. Resolving long-range spatial correlations in jammed colloidal systems using photon correlation imaging. *Phys. Rev. Lett.* **2009**, *102*, 085702.
- (10) Lieleg, O.; Kayser, J.; Brambilla, G.; Cipelletti, L.; Bausch, A. R. Slow dynamics and internal stress relaxation in bundled cytoskeletal networks. *Nat. Mater.* **2011**, *10*, 236–242.
- (11) Park, J. A.; Kim, J. H.; Bi, D.; Mitchel, J. A.; Qazvini, N. T.; Tantisira, K.; Park, C. Y.; McGill, M.; Kim, S.-H.; Gweon, B.; *et al.* Unjamming and cell shape in the asthmatic airway epithelium. *Nature Mater.* **2015**, *14*, 1040–1048.

- (12) Malinverno, C.; Corallino, S.; Giavazzi, F.; Bergert, M.; Li, Q.; Leoni, M.; Disanza, A.; Frittoli, E.; Oldani, A.; Martini, E.; *et al.* Endocytic reawakening of motility in jammed epithelia. *Nature Mater.* **2017**, doi: 10.1038/NMAT4848 (2017).
- (13) Bechinger, C.; Di Leonardo, R.; Lowen, H.; Reichhardt, C.; Volpe, G.; Volpe, G. Active particles in complex and crowded environments. *Rev. Mod. Phys.* **2016**, *88*, 045006.
- (14) Royall, C. P.; Williams, S. R. The role of local structure in dynamical arrest. *Phys. Rep.* **2015**, *560*, 1–75.
- (15) Tanaka, H. Importance of many-body orientational correlations in the physical description of liquids. *Faraday Discuss.* **2013**, *167*, 9–76.
- (16) Widmer-Cooper, A.; Perry, H.; Harrowell, P.; Reichman, D. R. Irreversible reorganization in a supercooled liquid originates from localized soft modes. *Nat. Phys.* **2008**, *4*, 711–715.
- (17) Manning, M. L.; Liu, A. J. Vibrational modes identify soft spots in a sheared disordered packing. *Phys. Rev. Lett.* **2011**, *107*, 108302.
- (18) Mosayebi, M.; Ilg, P.; Widmer-Cooper, A.; Del Gado, E. Soft modes and nonaffine rearrangements in the inherent structures of supercooled liquids. *Phys. Rev. Lett.* **2014**, *112*, 105503.
- (19) Tsamados, M.; Tanguy, A.; Goldenberg, C.; Barrat, J. L. Local elasticity map and plasticity in a model Lennard-Jones glass. *Phys. Rev. E* **2009**, *80*, 026112.
- (20) Starr, F. W.; Sastry, S.; Douglas, J. F.; Glotzer, S. C. What do we learn from the local geometry of glass-forming liquids? *Phys. Rev. Lett.* **2002**, *89*, 125501.
- (21) Candelier, R.; Widmer-Cooper, A.; Kummerfeld, J. K.; Dauchot, O.; Biroli, G.; Harrowell, P.; Reichman, D. R. Spatiotemporal hierarchy of relaxation events, dynamical

- heterogeneities, and structural reorganization in a supercooled liquid. *Phys. Rev. Lett.* **2010**, *105*, 135702.
- (22) Yu, H.-B.; Richert, R.; Samwer, K. Correlation between viscoelastic moduli and atomic rearrangements in metallic glasses. *J. Phys. Chem. Lett.* **2016**, *7*, 3747–3751.
- (23) Larini, L.; Ottochian, A.; De Michele, C.; Leporini, D. Universal scaling between structural relaxation and vibrational dynamics in glass-forming liquids and polymers. *Nat. Phys.* **2007**, *4*, 42–45.
- (24) Pastore, R., Coniglio, A.; Pica Ciamarra, M. From cage-jump motion to macroscopic diffusion in supercooled liquids. *Soft Matter* **2014**, *10*, 5724–5728.
- (25) Pastore, R.; Pesce, G.; Sasso, A.; Pica Ciamarra M. Connecting short and long time dynamics in hard-sphere-like colloidal glasses. *Soft Matter* **2015**, *11*, 622.
- (26) Pastore, R.; Coniglio, A.; Pica Ciamarra, M. Spatial correlations of elementary relaxation events in glass-forming liquids. *Soft Matter* **2015**, *11*, 7214–7218.
- (27) Pastore, R.; Coniglio, A.; de Candia, A.; Fierro, A.; Pica Ciamarra, M. Cage-jump motion reveals universal dynamics and non-universal structural features in glass forming liquids. *J. Stat. Mech.: Theory Exp.* **2016**, 054050.
- (28) Weeks, E. R.; Weitz, D. A. Properties of cage rearrangements observed near the colloidal glass transition. *Phys. Rev. Lett.* **2002**, *89*, 095704.
- (29) Chaudhuri, P.; Berthier, L.; Kob, W. Universal nature of particle displacements close to glass and jamming transitions. *Phys. Rev. Lett.* **2007**, *99*, 060604.
- (30) Pica Ciamarra, M.; Pastore R.; Coniglio A.; Particle jumps in structural glasses. *Soft Matter* **2016**, *12*, 358–366.
- (31) Vollmayr-Lee, K. Single particle jumps in a binary Lennard-Jones system below the glass transition. *J. Chem. Phys.* **2004**, *121*, 4781–4794.

- (32) Helfferich, J.; Ziebert, F.; Frey, S.; Meyer, H.; Farago, J.; Blumen, A.; Baschnagel, J.; Continuous-time random-walk approach to supercooled liquids. I. Different definitions of particle jumps and their consequences. *Phys. Rev. E*. **2014**, *89*, 042603.
- (33) Niblett, S. P.; de Souza, V. K.; Stevenson, J. D.; Wales, D. J.; Dynamics of a molecular glass former: Energy landscapes for diffusion in ortho-terphenyl. *J. Chem. Phys.* **2016**, *145*, 024505
- (34) Bernini, S.; D. Leporini. Cage effect in supercooled molecular liquids: Local anisotropies and collective solid-like response. *J. Chem. Phys.* **2016** , *44*, 144505.
- (35) Mirigian, S; Schweizer, K. S. Unified theory of activated relaxation in liquids over 14 decades in Time *J. Phys. Chem. Lett.* **2013**, *4*, 3648–3653
- (36) Gokhale, S.; Nagamanasa, K. H.; Ganapathy, R.; Sood, A. K. Growing dynamical facilitation on approaching the random pinning colloidal glass transition. *Nat. Commun.* **2014**, *5*, 4685.
- (37) Nagamanasa, K. H.; Gokhale, S.; Sood, A. K.; Ganapathy, R. Direct measurements of growing amorphous order and non-monotonic dynamic correlations in a colloidal glass-former. *Nat. Phys.* **2015**, *11*, 403–408.
- (38) Gokhale, S.; Ganapathy, R.; Nagamanasa, K. H.; Sood, A. K. Localized excitations and the morphology of cooperatively rearranging regions in a colloidal glass-forming Liquid. *Phys. Rev. Lett.*, **2016**, *116*, 068305.
- (39) Vivek, S.; Kelleher, C. P.; Chaikin, P. M.; Weeks, E. R. Long-wavelength fluctuations and the glass transition in two dimensions and three dimensions. *Proc. Natl. Acad. Sci. U. S. A.* **2017**, *114*, 1850–1855.
- (40) Plimpton, S. Fast parallel algorithms for short-range molecular dynamics. *J. Comput. Phys.* **1995**, *117*, 1–19.

- (41) Likos, C. N. Effective interactions in soft condensed matter physics. *Phys. Rep.* **2001**, *348*, 267–439.
- (42) Durian, D. J. Foam mechanics at the bubble scale. *Phys. Rev. Lett.* **1995**, *75*, 4780.
- (43) Paloli, D.; Mohanty, P. S.; Crassous, J. J.; Zaccarelli, E.; Schurtenberger, P. Fluid–solid transitions in soft–repulsive colloids. *Soft Matter* **2013**, *9*, 3000–3004.
- (44) Berthier, L.; Witten, T. A. Compressing nearly hard sphere fluids increases glass fragility. *Europhys. Lett.* **2009**, *86*, 10001.
- (45) Pastore, R.; Coniglio, A.; Pica Ciamarra, M.; Dynamic phase coexistence in glass–forming liquids. *Sci. Rep.* **2015**, *5*, 11770.
- (46) Mackowiak, S. A.; Kaufman, L. J. When the heterogeneous appears homogeneous: discrepant measures of heterogeneity in single-molecule observables. *J. Phys. Chem. Lett.* **2011**, *2*, 438–442.
- (47) Murray, C. A.; Wenk, R. A. Microscopic particle motions and topological defects in two-dimensional hexatics and dense fluids. *Phys. Rev. Lett.* **1989**, *62*, 1643–1646.
- (48) Patashinski, A. Z.; Ratner, M. A.; Grzybowski, B. A.; Orlik, R.; Mitus, A. C. Heterogeneous structure, heterogeneous dynamics, and complex behavior in two-dimensional Liquids. *J. Phys. Chem. Lett.* **2012**, *3*, 2431–2435.
- (49) Ramírez-González, P. E; López-Flores, L.; Acuña-Campa, H.; Medina-Noyola, M. Density-temperature-softness scaling of the dynamics of glass-forming soft-sphere liquids. *Phys. Rev. Lett.* **2011**, *107*, 155701.
- (50) López-Flores, L.; Mendoza-Méndez, P.; Sánchez-Díaz, L. E.; Yeomans-Reyna, L. L.; Vizcarra-Rendón, A.; Pérez-Ángel, G.; Chávez-Páez, M.; Medina-Noyola, M. Dynamic equivalence between atomic and colloidal liquids. *Europhys. Lett.* **2012**, *99*, 46001.

- (51) López-Flores, L.; Ruíz-Estrada, H.; Chávez-Páez, M.; Medina-Noyola, M. Dynamic equivalences in the hard-sphere dynamic universality class. *Phys. Rev. E* **2013**, *88*, 042301.
- (52) Dyre, J. C. Simple liquids´ quasiuniversality and the hard-sphere paradigm. *J. Phys.: Condens. Matter* **2016**, *28*, 323001.
- (53) Pica Ciamarra, M.; Sollich, P. Dynamics and instantaneous normal modes in a liquid with density anomalies. *Journ. Phys.: Condens. Matter* **2015** , *27*, 194128.